



## Finite element model analysis of thermal failure in connector

WANG Xin<sup>†</sup>, XU Liang-jun

(Research Lab of Electric Contacts, Beijing University of Posts & Telecommunications, Beijing 100876, China)

<sup>†</sup>E-mail: wangxin820117@gmail.com

Received Dec. 19, 2006; revision accepted Jan. 5, 2007

**Abstract:** Thermal analysis and thermal diagnose are important for small power connector especially in electronic devices since their structure is usually compact. In this paper thermal behavior of small power connector was investigated. It was found that the contact resistance increased due to the Joule heating, and that increased contact resistance produced more Joule heating; this mutual action causes the connector to lose efficiency. The thermal distribution in the connector was analyzed using finite element method (FEM). The failure mechanism is discussed. It provides basis for improving the structure. The conclusion was verified by experimental results.

**Key words:** Connector, Stress relaxation, Finite element method (FEM), Thermal failure

**doi:**10.1631/jzus.2007.A0397

**Document code:** A

**CLC number:** TB114.3; O224; O211.6

### INTRODUCTION

Connector is an electromechanical device, which provides a separable interface between two subsystems of an electronic system without bad effect on the performance of the system. With the development of electronic technologies, the connector type has increased to hundreds of species. At the same time, its design and manufacture tend to miniaturization, low height, narrow space, multifunction (Morita *et al.*, 1996).

Under working condition, the connector suffers from fretting and corrosion on the contact surface (Willamison, 1981). That could make the contact resistance increase and cause contact failure. Joule heating produced by  $I^2R$  increases as the contact resistance increases, causes temperature rise on the contact surface, then causes many problems (Yu and Li, 1977): (1) The contact surface at this high temperature will soften, melt or even boil, the material of the two contact surfaces will transfer to each other, and cause the contact surface to be destroyed. (2) The oxidation of the contact surface is accelerated. If some organic is close to it, it will decompose them, which will adversely impact the reliability of the contact. (3) Accelerate diffusion and formation of

non-metal film, and cause contact failure. (4) Spring connector to reduce the normal force of the contact, and unstablize it (Greenwood, 1966). Therefore, in the process of analyzing the contact failure, thermal study of the contact surface is very important.

In this paper, thermal analysis—thermal distribution and temperature increase of the connector was done using finite element method (FEM). The results were verified by experiments.

### STEADY-STATE THERMAL ANALYSIS OF THE CONNECTOR

For obtaining the connector's fretting behavior, two lab simulation experiments were done (Section V, Fig.5 and Table 6).

In order to get the temperature distribution inside the connector, FEM simulation was performed. The FEM of the connector (Fig.1) was created mainly based on blueprint (Fig.2).

The connector spring material was Cu-Sn6 (the material includes Sn 6% (w/w), Cu 94% (w/w)) with Sn plating; and the plug sheet was 45<sup>#</sup> steel with Ni plating. As the plating is very thin, it will not have obvious effect on the thermal analysis, and so, was



As we know, there are three possibilities of heat transmitting from the contact area: conduction, convection and radiation. For stationary cases, heat conduction is described by the following differential equation:

$$\lambda A \nabla^2 T = q, \quad (2)$$

where  $\lambda$  is thermal conduction coefficient;  $A$  is cross sectional area;  $T$  is temperature;  $q$  is heat production rate.

In the FEM-software, this equation is changed into a system of equations in matrix notation:

$$[\mathbf{K}]\{\mathbf{T}\}=\{\mathbf{q}\}, \quad (3)$$

where  $[\mathbf{K}]$  is matrix of heat conduction;  $\{\mathbf{T}\}$  is vector of temperatures;  $\{\mathbf{q}\}$  is vector of heat flow.

By solving these equations with FEM, the temperature distribution in the connector, due to heat conduction is obtained. The parameters of conductivity coefficients are listed in Table 1.

Convection, i.e. the heat transport between the model and its environment is calculated by:

$$\alpha A(T_F - T_W) = q, \quad (4)$$

where  $\alpha$  is heat convection coefficient;  $A$  is cross sectional area;  $T_F/T_W$  is temperature of the fluid/wall;  $q$  is heat flow.

Here the convection parameter used large space convection model (Li *et al.*, 1998). Large space means that there is no other interference in the convection around the structure. The convection factors are listed in Table A1 in Appendix A. According to the connector structure, the convection coefficient of the socket is calculated with Type I convection, the plug sheet convection coefficient is calculated with Type II convection.

Radiation is given by Stefan-Boltzmann's law:

$$A_i F_{ij} \varepsilon_i \sigma (T_i^4 - T_j^4) = q, \quad (5)$$

where  $A_i$  is area of emitter  $i$ ;  $F_{ij}$  is form factor between area  $i, j$ ;  $\varepsilon_i$  is degree of emission of area  $i$ ;  $\sigma$  is Stefan-Boltzmann constant;  $T_i/T_j$  is temperature of emitter area  $i$ /receiver  $j$  in Kelvin;  $q$  is heat flow.

In the analysis, radiation obviously exists be-

tween the socket and the plug sheet, therefore radiance is considered. The radiation parameters are listed in Table 3.

**Table 3 The HF of the experiment**

| Material            | Radiance |
|---------------------|----------|
| Socket (45# steel)  | 0.11     |
| Plug sheet (Cu-Sn6) | 0.18     |
| Housing (PA66)      | 0.90     |

## RESULT ANALYSIS

The analysis results are shown in Fig.4.

The result FEM analysis of Experiment 2 showed that the contact surface temperature is very high (330~380 °C), this value has gone far beyond the limitation of the spring material's acceptable temperature (150~175 °C) (Oberger and Olssen, 1996). When the connector works at this or higher temperature for a long time, stress relaxation will occur in the spring material (Robert, 1988). Because the normal contact force of the connector depends on the initial deformation of the spring, the contact force will reduce due to stress relaxation, and cause contact failure. The analysis results of Experiments 1 and 2 are listed in Table 4.

**Table 4 The analysis results of the experiment**

| Experiment No. | Temperature distribution range (°C) | Contact surface temperature (°C) |
|----------------|-------------------------------------|----------------------------------|
| 1              | 20.0~162.7                          | 120~140                          |
| 2              | 20.0~477.3                          | 330~380                          |

Table 4 shows that although the saturated contact resistance in Experiment 1 (300 mΩ) is far beyond the saturated contact resistance in Experiment 2 (100 mΩ), the temperature of the contact surface is not very high as the Joule heat of Experiment 1 is smaller than that of Experiment 2 (Table 5), which does not exceed the limited application temperature, so the contact can remain in good contact state also. While on the contrary, when the connector works at high current (as Experiment 2), the rise of the contact resistance makes the contact surface temperature very high, that will lead to contact failure and adversely impact the reliability of the contact. Therefore, in this case control of the contact temperature is very important to the connector.

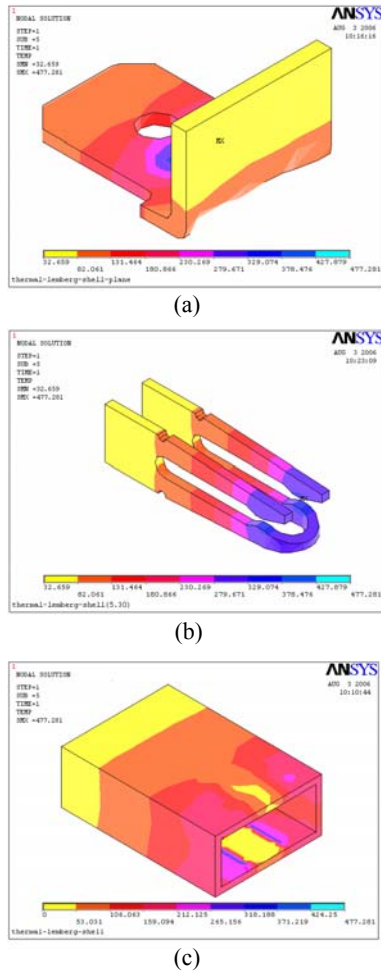


Fig.4 Temperature distribution of the plug sheet (a), the socket (b) and the housing (c)

HEAT BALANCE EQUATION

- (1) The heat power produced from contacts (Li et al., 1997):  $HG=I^2R$ .
- (2) The diffused heat by metal conduction:  $HD=K(T_m-T_0)=12\pi\lambda a(T_m-T_0)$ , where  $K$ , thermal conductivity;  $\lambda$ , thermal conductivity coefficient;  $a$ , radius of a-spot, supposing the contact zone is a circle spot.
- (3) The contact resistance:  $R_c=(\rho_1+\rho_2)/(4a)$ .
- (4) If  $HG=HD$ , the balanced contact resistance is:

$$R_c = \sqrt{\frac{12\pi\lambda(\rho_1 + \rho_2)(T_m - T_0)}{4I^2}} \tag{6}$$

The material parameters in this experiment are:

$\lambda_{Cu-Sn6}=75 \text{ W/(m}\cdot\text{K)}$ ,  $\lambda_{Fe}=45 \text{ W/(m}\cdot\text{K)}$ ,  $\rho_{Cu}=16.7\times 10^{-9} \Omega\cdot\text{m}$ ,  $\rho_{Sn}=114.9\times 10^{-9} \Omega\cdot\text{m}$ ,  $\rho_{Ni}=68.5\times 10^{-9} \Omega\cdot\text{m}$ ,  $\rho_{Fe}=97.1\times 10^{-9} \Omega\cdot\text{m}$ .

By Eq.(6), FEM results and calculation results of the rising temperature on the contact surface are listed in Table 5.

Table 5 Calculation results and FEM results (°C)

| Experiment No. | Calculation results | FEM results | Difference | Deviation |
|----------------|---------------------|-------------|------------|-----------|
| 1              | 104.40              | 117.33      | 12.93      | 11.6      |
| 2              | 310.26              | 332.35      | 22.09      | 6.9       |

We can see that calculation results are always lower than FEM results, mainly because the heat balance equation does not take radiation and convection into account. However, the deviation of calculation results and FEM results is low (<10%), so we can say the FEM result is acceptable.

ANALYSIS OF THE EXPERIMENT

In the fretting lab simulation experiment, the connection resistance (four paralleled contacts) was monitored (Fig.5). The amplitude of micro-motion is 200  $\mu\text{m}$ , frequency is 2 Hz, and current load is set 2 and 6 A respectively, the open circuit voltage is 10~20 V. These experiment conditions show the influence of fretting on connection resistance. The average connection resistance when it tended to be saturated and time to reach this value are listed in Table 6.

Temperature was tested to verify the calculation results of FEM (Fig.6). Temperature sensor was Pt100 in temperature measurement.

Pt100 is connected to HP multi-meter to get the temperature data. Meantime, the resistance data can also be obtained from computer.

The testing results and FEM results are listed in Table 7 showing that FEM analysis results are consistent with testing data.

ANALYSIS AND DISCUSSION

Fig.7 shows the experimental result of the relationship between Joule heat and current load. It can be seen that when current load increases, contact resistance reduces due to softening of contact material. So

Joule heat is combination result of increased current and decreased contact resistance.

For most contact material, when temperature increases above 150~175°C, its stress relaxation will be accelerated. Therefore, the temperature increase of the contact surface plays a very important role in the contact reliability. Especially for high current load through the contact, the thermal energy dissipation of the inside of the connector should be carefully designed in such a way that the air convection of the inside of the connector is improved, good contact environment is maintained to avoid contact surface corrosion.

The above analysis also shows that the FEM analysis can accurately simulate the actual temperature distribution of the connectors, and could be a good CAE tool for the connector.

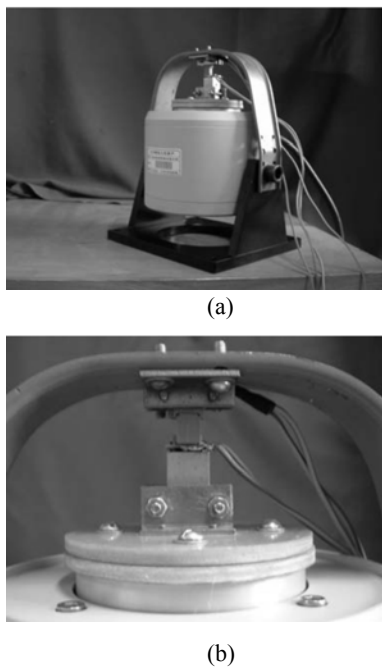


Fig.5 The experimental equipment

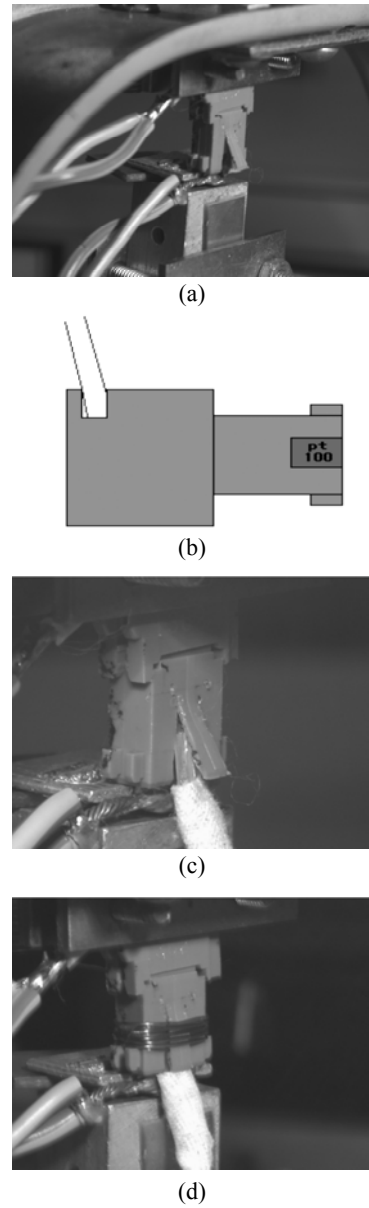


Fig.6 Temperature was tested to verify the calculation results of FEM. (a) The slot on the housing; (b) Measurement position of the connector; (c) Installs the Pt100; (d) Fix the Pt100

Table 6 Experimental conditions and results

| Experiment No. | Materials   | Current | Open voltage | Frequency | Amplitude | Total testing time |
|----------------|-------------|---------|--------------|-----------|-----------|--------------------|
| 1              | Sn/Cu-Ni/Fe | 2       | 10           | 2         | 200       | 1                  |
| 2              | Sn/Cu-Ni/Fe | 6       | 10           | 2         | 200       | 2                  |

Table 7 FEM results and experimental results

| Experiment No. | Calculation results (°C) | FEM results (°C) | Difference (°C) | Deviation (°C) |
|----------------|--------------------------|------------------|-----------------|----------------|
| 1              | 49.45                    | 45.69            | 3.76            | 7.9            |
| 2              | 87.99                    | 87.70            | 0.29            | 0.3            |

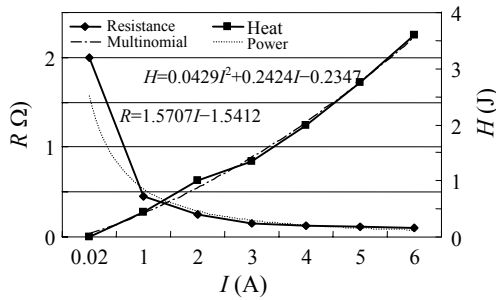


Fig.7 Joule heat increased with currents

CONCLUSION

This paper makes a steady-state thermal analysis on the connector by the use of ANSYS 6.0, the analysis is shown below.

(1) When the connector works under high current load, the rise of the contact resistance gets the temperature of the contact surface high, this has gone far beyond the limitation of the spring material's application temperature. If connector works in this temperature or even higher in a long time, the stress relaxation will occur in spring material, which will lead to contact failure and impact the reliability of the contact, and even make connector burned out (Internal Reports, 2006).

(2) Through comparing the FEM analysis results with the experimental results, we can see that they have a better consistency.

(3) In the case of the high current load connector, it must have a good contact; the contact resistance

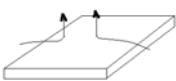
should be low and stable (Singer, 1991). In the process of the design of this connector, the temperature control of the connector is very important.

References

Greenwood, A., 1966. Contact of Nominally Flat Surface, Proceeding of the Royal Society, p.295.  
 Internal Reports, 2006. Research Report of Failure Analysis on the Burned Connectors.  
 Li, K., Lu, J.G., Zhang, G.S., 1997. Mathematical analysis of thermal process of static electrical contacts. *High Voltage Apparatus*, **1**:134.  
 Li, K., Su, X.P., Li, Z.G., Lu, J.G., Zhang, G.S., 1998. The Finite-Element Model and Analysis of Static Contact Resistance and Thermal Process for Contact with Film. Proc. 44th IEEE Holm Conf., p.226-229.  
 Morita, T., Ohuchi, K., Kaji, M., 1996. Numerical Model of Crimping by Finite Element Method. Proc. 42th IEEE Holm Conf., p.151-155.  
 Oberg, A., Olssen, K.E., 1996. Computer Simulation of the Influence of Intermetallics on the Stability of Electrical Contacts. Proc. 42th IEEE Holm Conf., p.137.  
 Robert, D.M., 1988. Multispot Model of Contacts Based on Surface Features. The 34th Holm Conference on Electrical Contact, p.256.  
 Schedin, E., Thuvander, A., Henderson, P., Sandberg, P., Kamf, A., 1996. Stress Relaxation Behaviour of Connectors—Development of Simulation Techniques. Proc. 42th IEEE Holm Conf., p.142.  
 Singer, M.T., 1991. Electrical resistance of random rough contacting surfaces using fractal surface modeling the contact interface. *IEEE Trans. on CHMT*, **14**(1):89-93.  
 Willamison, B.J.P., 1981. The Microworld of the Contact Spot, The 27th Holm Conference on Electrical Contact, p.245.  
 Yu, H.Y., Li, J.C., 1977. Computer simulation of impression creep by the finite element method. *Journal of Materials Science*, **12**(11):2214-2222. [doi:10.1007/BF00552243]

APPENDIX A

Table A Convection coefficient of the experiment

| Convection form number | Surface shape                | Convection form   | Convection coefficient equation | Convection coefficient (W/(m <sup>2</sup> ·K)) (Δt=1°C) |
|------------------------|------------------------------|---|---------------------------------|---|
| I                      | Erect plane and erect column |  | $\alpha=1.10(\Delta t/l)^{1/4}$ | 3.35  |
| II                     | Level plane                  |  | $\alpha=1.01(\Delta t/l)^{1/4}$ | 3.68  |

Note: (1) Δt is the temperature difference between objects and fluid; l is the stereotypes size; (2) The applicable condition of the equation: air temperature 10~40 °C, surface temperature 50~100 °C